Hydroxyl radical-induced apoptosis in human tumor cells is associated with telomere shortening but not telomerase inhibition and caspase activation

Jian-Guo Ren[a], Hui-Li Xia[a], Tom Just[b], Yao-Ren Dai[a,*]

[a] *Department of Biological Sciences and Biotechnology, Tsinghua University, Beijing 100084, PR China*
[b] *Department of Probe Applications, DAKO A/S, Produktionsvej 42, DK-2600 Glostrup, Denmark*

Received 25 August 2000; revised 1 December 2000; accepted 4 December 2000

First published online 2 January 2001

Edited by Veli-Pekka Lehto

Abstract Reactive oxygen species (ROS) have been found to trigger apoptosis in tumor cells. At the same time, telomerase is found to be associated with malignancy and reduced apoptosis. However little is known about the linkage between ROS such as •OH and telomerase/telomere. To address the interrelations between •OH and telomerase/telomere in tumor cell killing, HeLa, 293 and MW451 cells were induced to undergo apoptosis with •OH radicals generated via Fe^{2+}-mediated Fenton reactions (0.1 mM $FeSO_4$ plus 0.3–0.9 mM H_2O_2) and telomerase activity, telomere length were measured during apoptosis. We found that during •OH-induced apoptosis, telomere shortening took place while no changes in telomerase activity were observed. Our results suggest that •OH-induced telomere shortening is not through telomerase inhibition but possibly a direct effect of •OH on telomeres themselves indicating that telomere shortening but not telomerase inhibition is the primary event during •OH-induced apoptosis. Strikingly, we also found that •OH-induced apoptosis in HeLa cells is caspase-3-independent but is associated with reduction of mitochondrial transmembrane potential. Our results indicate that •OH triggers apoptotic tumor cell death through a telomere-related, caspase-independent pathway.

Key words: Telomere; Telomerase; Hydroxyl radical; Caspase; Reactive oxygen species; Mitochondrial transmembrane potential

1. Introduction

Reactive oxygen species (ROS) generation has been found to be an important event in apoptotic tumor cell death induced by various anti-cancer agents such as camptothecin, vinblastine, inostamycin and adrimycin [1]. On the other hand, ROS scavengers such as *N*-acetyl-L-cysteine and glutathione (GSH) have been found to inhibit apoptosis induced by TGFβ-1, TNF-α and growth factor deprivation in IL-3-dependent murine pro-B lymphocyte, murine T cell hybridoma, human ovarian carcinoma and Hit cells [2–4]. Hence exploration of the mechanism underlying ROS-triggered apoptosis in tumor cells is crucial to our understanding of the chemotherapeutic effect of anti-cancer drugs.

At the same time, telomerase has become a potential target for anti-cancer therapeutic application based on the strong correlation between telomerase activity and malignancy [5]. Furthermore, it was found that inhibition of telomerase either by oligonucleotides against human telomerase RNA or via dominant-negative mutants of hTERT (human telomerase reverse transcriptase) in human tumor cells leads to progressive telomere shortening and apoptotic cell death [6,7]. In human fibroblasts, rate of telomere shortening was increased by mild hyperoxia and hydrogen peroxide [8,9]. It is thus intriguing to study the interrelation between ROS action and telomere/telomerase during apoptosis.

Moreover, in recent years mitochondria have been found to play a specific role in apoptosis. At least three mitochondrial events, including loss of mitochondrial transmembrane potential ($\Delta\Psi_m$), induction of mitochondrial permeability transition (MPT), and cytosolic translocation of cytochrome *c* which participates in the activation of caspase-3, have been found to be essential components of the apoptotic pathway [10–15]. Moreover, advanced telomere shortening was reported in blood cells from patients with respiratory chain disorders [16].

To investigate the mechanism during anti-cancer agent-induced tumor cell death, HeLa, 293 and MW451 cells were induced to undergo apoptosis with hydroxyl radicals (•OH) generated directly via Fe^{2+}-mediated Fenton reaction and the changes in telomerase activity and telomere length during apoptosis and their relations to mitochondria-related apoptotic pathway were studied. We found that •OH caused severe telomere shortening while with no effect on telomerase activity and induced loss of $\Delta\Psi_m$ in the absence of caspase activation.

Our study provided evidence for the decisive and central role of ROS in a telomere-related, caspase-independent apoptotic pathway in human tumor cells. To our knowledge this is the first report about the linkage between •OH and telomere shortening and telomerase activity during apoptosis.

*Corresponding author. Fax: (86)-10-62785505.
E-mail: zhaizhh@mail.tsinghua.edu.cn

Abbreviations: TUNEL, terminal deoxynucleotidyltransferase (TdT)-mediated dUTP nick end labeling; DAPI, 4′,6-diamidino-2-phenylindole; ROS, reactive oxygen species; GSH, glutathione; $\Delta\Psi_m$, mitochondrial transmembrane potential; Ac-DEVD-CHO, Ac-Asp-Glu-Val-Asp-acid aldehyde; DODCB, 3,3′-diethyloxadicarbocyanine; Di-OC_6(3), 3,3′-dihexyloxacarbocyanine iodide; Rh 123, rhodamine 123; •OH, hydroxyl radical; MPT pore, mitochondrial permeability transition pore

PII: S0014-5793(00)02377-2

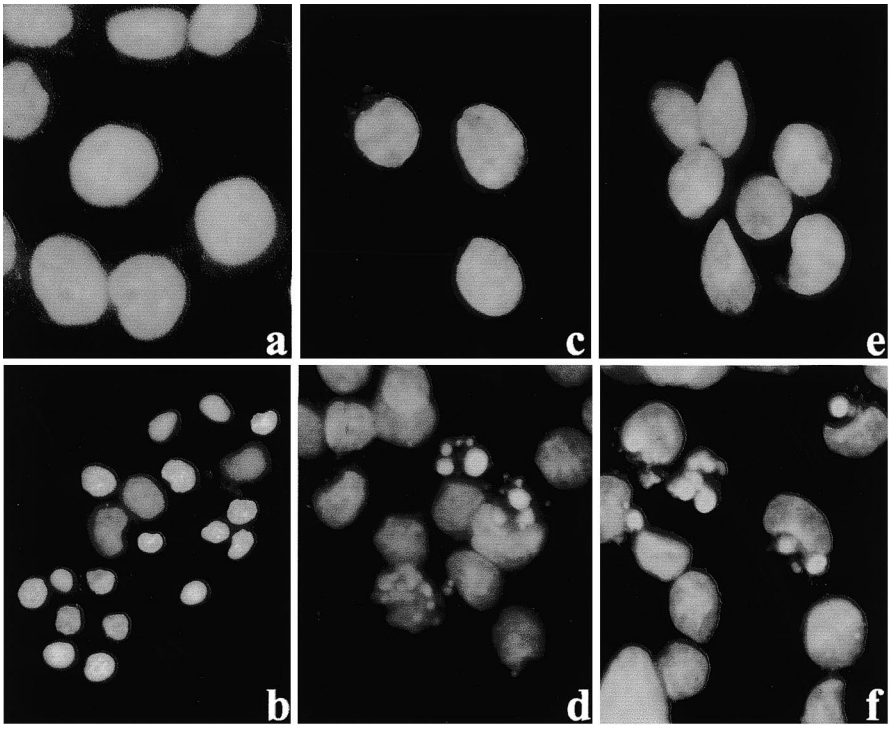

Fig. 1. Detection of apoptosis with DAPI in HeLa, MW451 and 293 cells. Cells were treated with 0.1 mM $FeSO_4$/0.6 mM H_2O_2 for 24 h, then stained with DAPI and observed under fluorescence microscope. (a, c, e) Control. (b, d, f) •OH-treated cells (×725).

2. Materials and methods

2.1. Materials

3,3′-Diethyloxadicarbocyanine (DODCB), pepstatin A, leupeptin, GSH, rhodamine 123 (Rh 123), 4′,6-diamidino-2-phenylindole (DAPI), ethidium bromide, 3,3′-dihexyloxacarbocyanine iodide (Di-OC_6(3)), Ac-Asp-Glu-Val-Asp-acid aldehyde (Ac-DEVD-CHO), glutaraldehyde, propidium iodide and osmium tetroxide were purchased from Sigma. 1,4-Dithiothreitol (DTT) was from Promega. Other substances were from commercial sources and of analytical grade. TUNEL (terminal deoxynucleotidyltransferase (TdT)-mediated dUTP nick end labeling) kit and telomerase assay kit were purchased from Boehringer Mannheim. All cell culture reagents were purchased from Gibco.

The $(CCCTAA)_3$ PNA probe was synthesized using the Expedite 8909 Nucleic Acid Synthesis System (PerSeptive Biosystems, Framingham, MA, USA) and was labeled at both the N- and C-termini with lysine-(5(6)-carboxyfluorescein). The probe was purified by reverse phase high performance liquid chromatography at 50°C and characterized by matrix-assisted laser desorption ionization time-of-flight mass spectrometry on a Hewlett Packard G 2025 A mass spectrometer (Hewlett Packard, San Fernando, CA, USA).

2.2. Cell culture

HeLa and 293 cells were seeded at 1×10^5 cells per culture flask in 10 ml of DMEM, MW451 cells were seeded at 1×10^5 cells per culture flask in 10 ml of RPMI 1640. All complete culture media contain 10% fetal calf serum, 100 μg/ml of streptomycin, and 100 U/ml of penicillin. Cells were incubated at 37°C in a humidified atmosphere containing 5% CO_2. Exponentially growing cells were used for experiments.

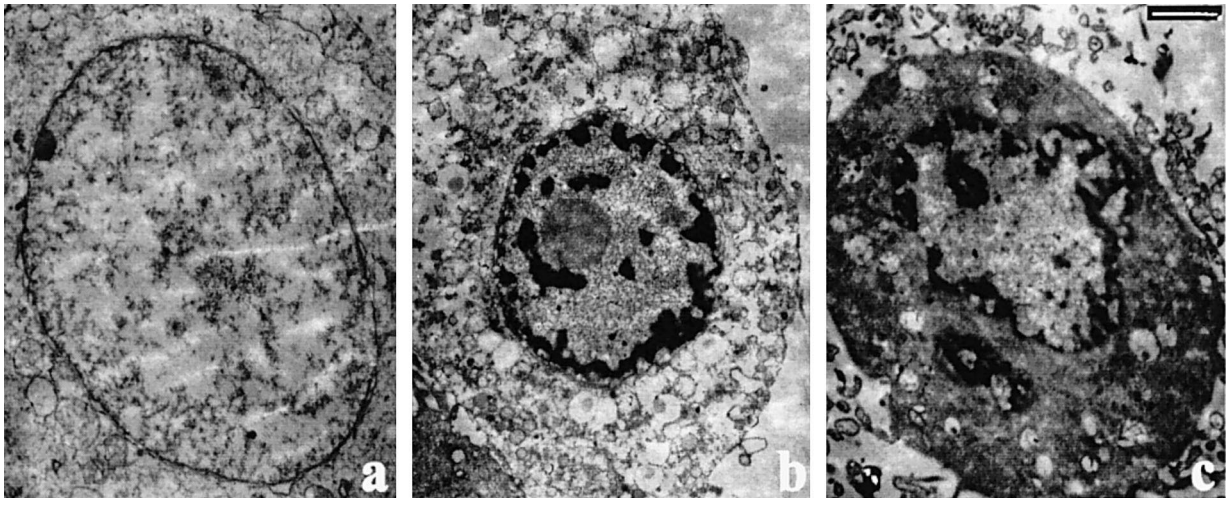

Fig. 2. Electron micrograph of HeLa cells undergoing apoptosis after treated by •OH for 24 h. (a) Control cells. (b, c) Cells treated with 0.1 mM $FeSO_4$/0.6 mM H_2O_2 showing chromatin condensation (b) and peripheral distribution (c). Bar, 2 μm.

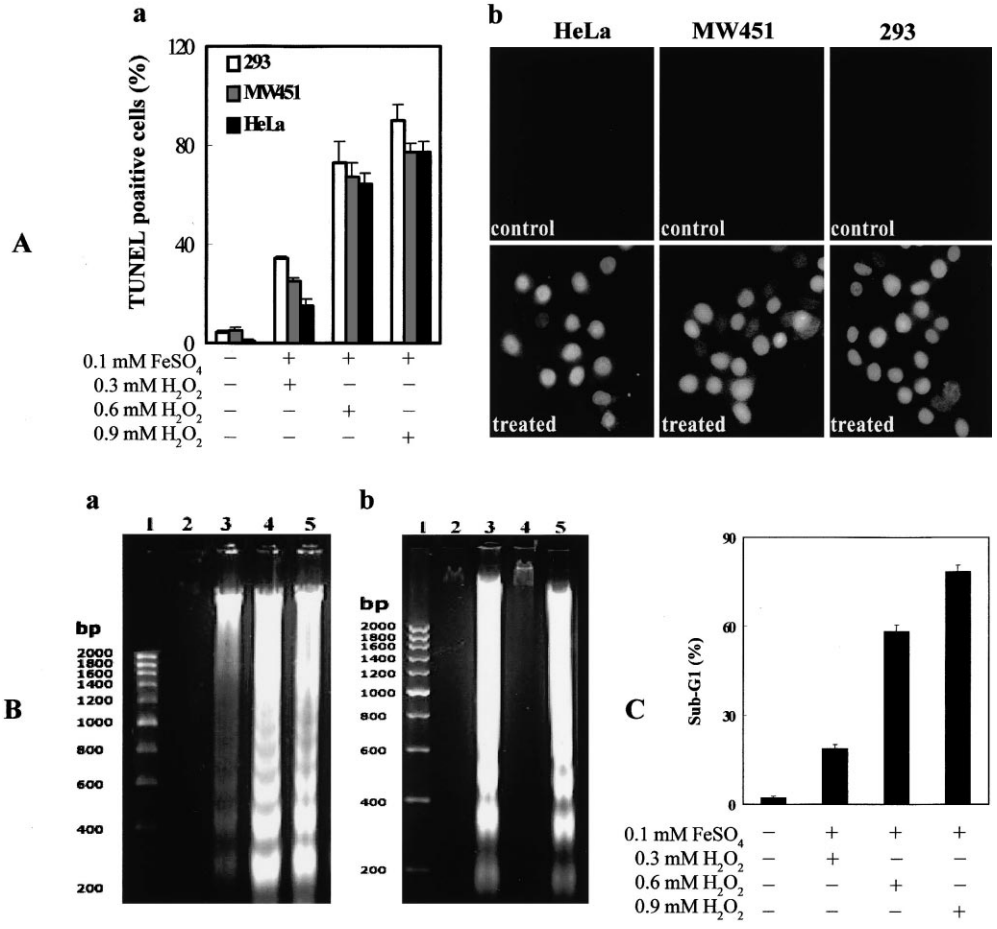

Fig. 3. Apoptosis in HeLa, MW451, and 293 cells. A: The TUNEL assay. (a) Percentage of TUNEL positive cells as determined after a 24 h •OH treatment. Values are the means ± S.D. of determinations from three separate experiments done in triplicates. Error bars indicate standard deviations. (b) In situ detection of DNA cleavage in HeLa, MW451 and 293 cells treated with 0.1 mM $FeSO_4$/0.6 mM H_2O_2. B: DNA laddering in •OH-treated HeLa, MW451 and 293 cells. (a) HeLa cells were treated with 0.1 mM $FeSO_4$ combined with 0.3 mM (lane 3), 0.6 mM (lane 4), and 0.9 mM (lane 5) H_2O_2 for 24 h, respectively; lane 1: markers; lane 2: control. (b) MW451 and 293 cells were treated with 0.1 mM $FeSO_4$/0.6 mM H_2O_2 for 24 h. lane 1: markers; lane 2: MW451 control; lane 3: DNA from •OH-treated MW451 cells; lane 4: 293 control; lane 5: DNA from •OH-treated 293 cells. C: Quantitative analysis of •OH-induced apoptosis in HeLa cells by flow cytometric analysis. Values are the means of three independent experiments done in triplicates. Error bars indicate standard deviations.

2.3. Induction of apoptosis and experiment treatments

•OH radicals were generated through the reaction of 0.1 mM $FeSO_4$ and 0.1, 0.3, 0.6, or 0.9 mM H_2O_2 and were used for apoptosis induction for the indicated length of time (from 0 to 24 h).

For telomerase inhibition, cells were preincubated with different concentrations of DODCB for 1 h before •OH treatment and remained in the medium afterwards. In the experiments using GSH, cells were pretreated with 1–10 mM GSH for 1 h before apoptosis induction. For caspase-3 inhibitor treatment, Ac-DEVD-CHO was added to the medium for 1 h followed by •OH treatment.

2.4. Electron microscopic (EM) observation

For EM analysis, cells were harvested and fixed in 2% glutaraldehyde in 0.05 M phosphate buffer, 0.05 M sucrose, pH 7.3 for 2 h at room temperature. Cells were then postfixed for 1 h in 1% osmium tetroxide, dehydrated through a graded series of ethanols, infiltrated, and embedded in Epon. 70 nm sections were collected onto copper grids, double-stained with oranyl acetate and lead citrate and examined in a Philips CM 120 transmission electron microscope.

2.5. DAPI staining

Cells were seeded 24 h before $FeSO_4$–H_2O_2 treatment onto glass coverslips, precoated with 1 mg/ml of poly-L-lysine (Sigma, M_r 3.7×10^4) at the density of 3×10^4 cells/cm^2. The cells were rinsed in D-Hanks' and fixed with methanol. After another rinse, cells were stained with 1 μg/ml DAPI (Sigma) in phosphate-buffered saline (PBS) for 30 min and counted. Apoptotic cells were determined by evaluating nuclear morphology using a fluorescence microscope (Nikon FLUOPHOT).

2.6. In situ detection of DNA cleavage by the TUNEL procedure

Apoptotic cells were also determined using a TUNEL kit (Boehringer Mannheim) as described by Gavrieli et al. [17]. Briefly, cells were plated on glass coverslips and incubated for different periods of time in medium with or without $FeSO_4/H_2O_2$. Cells were then fixed in freshly prepared paraformaldehyde solution (4% in D-Hanks', pH 7.4) for 30 min at room temperature. After rinsed with D-Hanks', cells were permeabilized with 0.1% Triton X-100 in 0.1% sodium citrate buffer and incubated for 1 h at 37°C with TdT and fluorescein isothiocyanate-dUTP to label the cleaved DNA. After that, coverslips were mounted in anti-fade mounting solution and observed under a fluorescence microscope (Nikon FLUOPHOT).

2.7. DNA laddering assay

For the DNA laddering assay, low molecular size DNA was isolated according to the method of Mandal et al. [18]. Briefly, cells collected were washed three times with PBS, and resuspended in 1 ml of lysis buffer (20 mM Tris–HCl, pH 8.0, 10 mM EDTA, pH 8.0, and 0.5% Triton X-100). After a 90 min incubation on ice, the lysates were centrifuged at $12\,000\times g$ for 10 min. Low molecular size DNA in the supernatant was extracted with an equal volume of phenol/chloroform for 1 h at 4°C. Ammonium acetate (2 M) was added

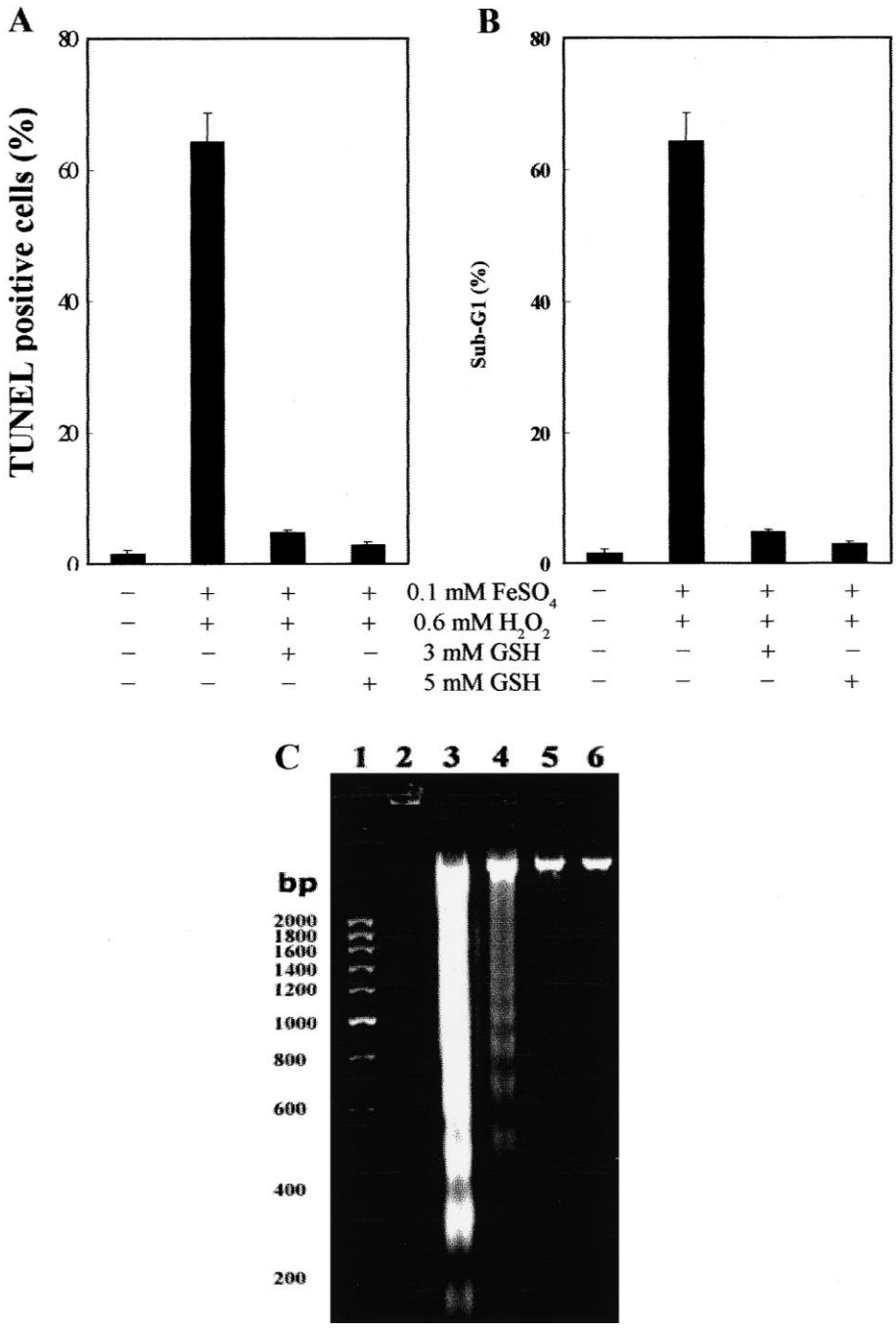

Fig. 4. Effect of GSH on •OH-induced apoptosis in HeLa cells as detected by the TUNEL procedure, flow cytometric analysis, and DNA laddering assay. Cells were preincubated with GSH for 1 h before a 24 h •OH treatment. A: Percentage of TUNEL positive cells. B: Percentage of Sub-G1 cells. Values are the means ± S.D. of three independent experiments done in triplicates. Error bars indicate standard deviations. C: DNA laddering in cells pretreated with GSH followed by 0.1 mM $FeSO_4$/0.6 mM H_2O_2 treatment. Lane 1: markers; lane 2: control; lane 3: DNA from •OH-treated cells; lanes 4–6: DNA from cells pretreated with 1 mM, 3 mM and 5 mM GSH, respectively.

to the aqueous phase, and DNA was precipitated with two volumes of ethanol at −20°C overnight. DNA was then treated with RNase A (1 mg/ml) at 37°C for 1 h, and total DNA was analyzed using 1.5% agarose gel electrophoresis. DNA fragments were visualized using ethidium bromide staining.

2.8. Flow cytometry

Flow cytometry measurements were carried out according to the methods described by Ishibashi et al. [19]. About 1×10^6 HeLa cells were fixed in 70% ethanol and then incubated in 1 ml PBS containing 50 μg/ml propidium iodide and 250 μg/ml RNase A (Boehringer Mannheim) at 37°C for 30 min. The fluorescence intensity was measured using a Coulter Elite Flow Cytometer. For each sample, 20 000 cells were analyzed using the Coulter Elite workstation 4.0 software (Coulter Corp.).

2.9. Detection of telomerase activity

Telomerase activity was measured using a PCR-based telomeric repeat amplification protocol (TRAP) enzyme-linked immunosorbent assay (ELISA) kit (Boehringer Mannheim) according to the manufacturer's description with some modifications. In brief, approximately 1×10^6 cells were lysed in 200 μl lysis reagent and incubated on ice for 30 min. For conducting TRAP reaction, 2 μl of cell extract (containing 2 μg protein) was added to 25 μl of reaction mixture and then an

appropriate amount of sterile water was added to make a final volume of 50 μl. PCR was performed in a PTC-100™ Programmable Thermal Controller (MJ Research, Inc.) as follows: primer elongation (30 min, 25°C), telomerase inactivation (5 min, 94°C), product amplification by repeat of 30 cycles (94°C for 30 s, 50°C for 30 s, 72°C for 90 s). Hybridization and ELISA reaction were carried out following manufacturer's instruction.

The extract from normal human fibroblasts served as negative controls. The extract of 293 cells was used as positive controls.

2.10. Measurement of telomere length

Fluorescence in situ hybridization was carried out following the procedure described by Hultdin et al. [20] and Rufer et al. [21] with some modifications. Trypsinized HeLa cells were harvested and washed with ice-cold PBS, centrifuged at $500\times g$ for 5 min and resuspended in 1 ml PBS. Typically, 5×10^5 cells (each sample was divided equally into two Eppendorf tubes) were used per tube. After centrifugation at $4900\times g$ for 30 s, the pellets were resuspended in a hybridization mixture containing 70% formamide (Fluka BioChemika, Buchs, Switzerland), 1% blocking reagent(Boehringer Mannheim GmbH, Mannheim, Germany) and fluorescein-$(CCCTAA)_3$-fluorescein PNA probe synthesized using the Expedite 8909 Nucleic Acid Synthesis System (PerSeptive Biosystems, Framingham, MA, USA) in 10 mM Tris pH 7.2. The volume of the hybridization mixture was adjusted to 100 μl/10^5 cells. Samples were heated for DNA denaturation for 10 min at 82°C followed by hybridization in the dark at room temperature overnight, the cells were centrifuged and washed twice in PBS at 40°C. Cells were then resuspended in PBS containing RNase A at 10 μg/ml (Boehringer Mannheim) and propidium iodide at 0.1 μg/ml, vortexing and incubated for 2–4 h at room temperature and analyzed immediately with a Coulter Elite Flow Cytometer or stored at 4°C for up to 2 days prior to analysis. For flow cytometric analysis, the FL_1 channel was used for detection of fluorescein signal and the FL_3 channel was for propidium iodide. List mode data from 1×10^4 cells in each experiment were collected and analyzed using Coulter Elite workstation 4.0 software (Coulter Corp.). The telomere fluorescence signal was defined as the mean fluorescence signal in cells after substraction of the background fluorescence signal.

2.11. Assay of caspase-3 activity

To measure caspase-3 activity, HeLa cells were harvested and washed once with ice-cold D-Hanks' and then resuspended in hypotonic cell lysis buffer (25 mM HEPES pH 7.5, 5 mM $MgCl_2$, 5 mM EDTA, 5 mM DTT, 2 mM PMSF, 10 μg/ml pepstatin A, 10 μg/ml leupeptin) at a concentration of 10^8 cells/ml, cells were lysed by four cycles of freezing and thawing, cell lysates were then centrifuged at $16\,000\times g$ for 20 min at 4°C and the supernatant fraction was collected. Caspase-3 activity was measured using a caspaACE™ Assay system, Fluorometric kit (Promega), following the manufacturer's description. Fluorescence intensity was measured with a fluorescence spectrophotometer at an excitation wavelength of 360 nm and an emission wavelength of 460 nm.

2.12. Measurement of mitochondrial transmembrane potential

$\Delta\Psi_m$ was measured according to the method of Yang et al. [22]. In brief, cells were incubated for 30 min in DMEM medium containing 5 μM Rh 123 and were then washed with Locke's buffer (154 mM NaCl, 5.6 mM KCl, 2.3 mM $CaCl_2$, 1 mM $MgCl_2$, 3.6 mM $NaHCO_3$, 5 mM glucose, 5 mM HEPES, pH 7.2). Cellular fluorescence was imaged using a confocal laser scanning microscope (MRC-1024, Bio-Rad) with excitation at 488 nm and emission at 530 nm. The objective lens was a 100× numerical aperture 1.4 PlanApo lens. The aperture size of the pinhole was 10∼40 nm. Confocal optical sections were less than 1 mm in thickness. Cells were selected randomly under bright-field optics and then scanned with the laser. Cellular fluorescence levels were quantified using both Rh 123 and Di-$OC_6(3)$ according to the method of Liu et al. [23] and McDonald et al. [24] by flow cytometry (Coulter Elite Flow Cytometer).

2.13. Statistical analysis

Data are expressed as means ± S.D. Significance was assessed by two tailed Student's *t*-test or one-way analysis of variance (ANOVA). All data represent at least three independent experiments performed in triplicates.

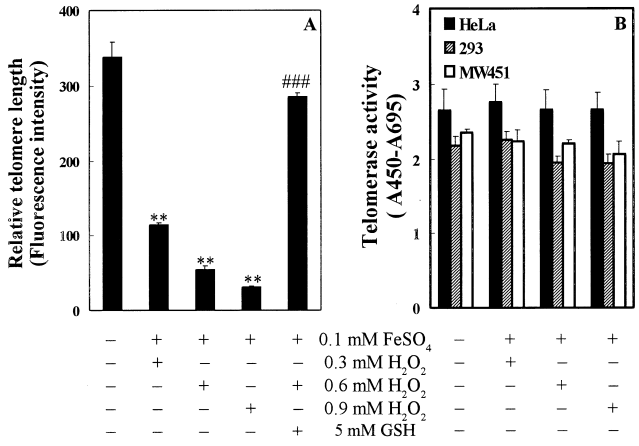

Fig. 5. Effect of •OH treatment on telomere length and telomerase activity. A: Telomere length was determined by the method of fluorescence in situ hybridization in •OH-treated HeLa cells with or without GSH pretreatment. B: Telomerase activities in HeLa, MW451 and 293 cells during apoptosis induction by •OH treatment. Values are means ± S.D. of three separate experiments done in triplicates. Error bars indicate standard deviations. $^{**}P<0.01$ compared with the untreated group and $^{###}P<0.001$ compared with the 0.1 mM $FeSO_4$/0.6 mM H_2O_2-treated group.

3. Results

3.1. Hydroxyl radicals induce apoptosis in human tumor cells

Human tumor cells including HeLa, MW451, and 293 cells demonstrated typical morphological and biochemical changes of apoptotic cells when treated with hydroxyl radicals generated via the Fe^{2+}-mediated Fenton reaction. Cells treated with •OH rounded up and lost their contact with surrounding cells and finally detached from the surface of culture flasks while control cells showed normal morphology. DAPI staining showed disintegration in nuclei of apoptotic HeLa, MW451 and 293 cells (Fig. 1). The apoptotic changes in nuclei including condensation and peripheral distribution of chromatin characteristic of apoptotic cells are further evidenced by EM observations (Fig. 2).

Moreover, the TUNEL procedure which detects cleavage of DNA in situ (Fig. 3A) and the assay of DNA laddering (Fig. 3B) which detects internucleosomal DNA degradation showed the apoptosis-specific DNA fragmentation in •OH-induced human tumor cell death. The flow cytometric analysis provided similar results (Fig. 3C).

The results indicate that exogenous •OH induces typical apoptosis in three human tumor cell lines used in this study.

3.2. •OH-induced HeLa cell death was rescued by GSH

When HeLa cells were preincubated with GSH (3 mM, 5 mM), a well-known antioxidant which scavenges free radicals in both in vivo and in vitro systems, for 1 h, the induction of apoptosis by •OH was almost completely eliminated as shown in Fig. 4. The results thus provided evidence for the involvement of •OH in apoptosis induction.

3.3. •OH induces telomere shortening but has no effect on telomerase activity in human tumor cells

Telomere shortening has been found to account for the

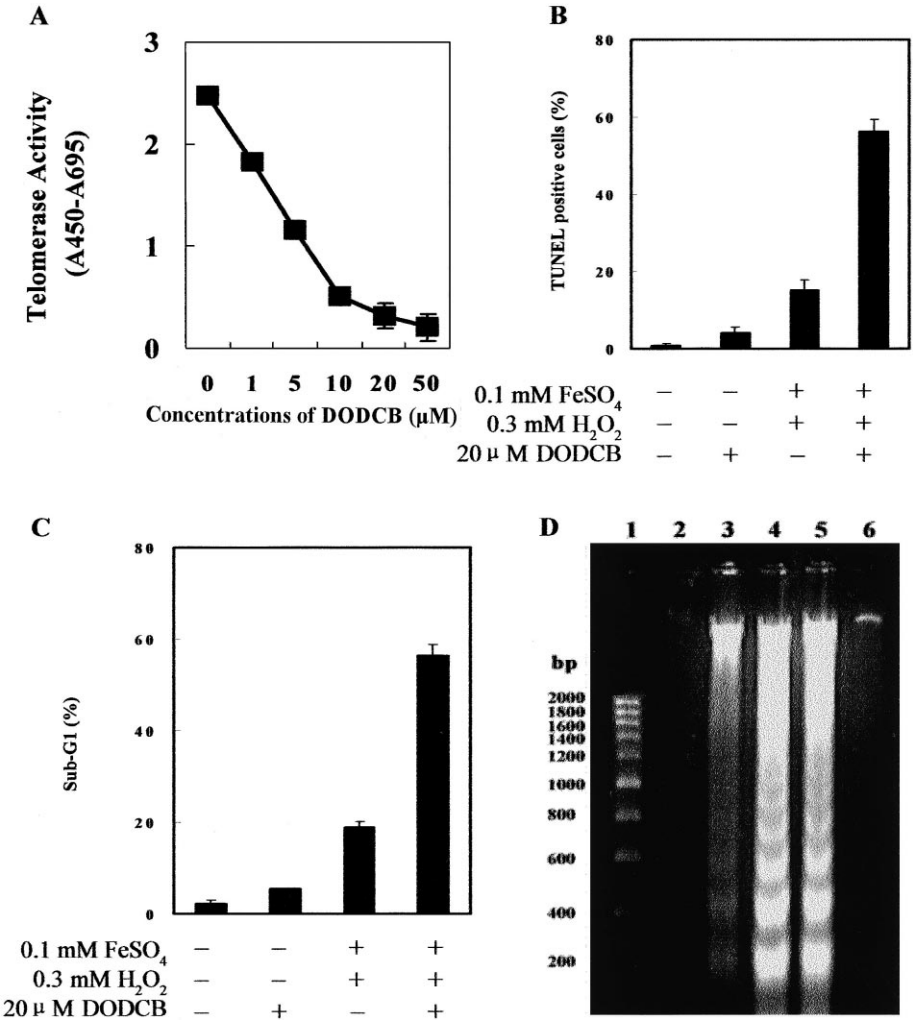

Fig. 6. Enhancement of apoptotic cell death in •OH-treated HeLa cells by DODCB, a telomerase inhibitor. Cells were preincubated with 20 μM DODCB for 1 h followed by a 24 h 0.1 mM $FeSO_4$/0.3 mM H_2O_2 or 0.1 mM $FeSO_4$/0.6 mM H_2O_2 treatment. A: Telomerase activity in cells treated with different concentrations of DODCB. B: Apoptosis detected by the TUNEL procedure. C: Flow cytometric analysis. D: DNA laddering assay. Lane 1, markers; lane 2, control; lane 3, DNA from 0.1 mM $FeSO_4$/0.3 mM H_2O_2-treated cells; lane 4, DNA from 0.1 mM $FeSO_4$/0.6 mM H_2O_2-treated cells. Lane 5, DNA laddering in cells pretreated with 20 μM DODCB followed by 0.1 mM $FeSO_4$/0.3 mM H_2O_2 treatment. Lane 6, DNA from 20 μM DODCB-treated cells. Values are means ± S.D. of three separate experiments done in triplicates. Error bars indicate standard deviations.

limitation of the numbers of divisions in normal human fibroblasts where telomerase activity is not detectable leading to cellular senescence. Recently, telomere shortening was also found to take place when immortalized human mammary epithelial cells were treated with telomerase inhibitors such as 2′-*O*-MeRNA(2). In this study, we investigated the interrelation between telomeres and hydroxyl radical-induced apoptosis and found that telomere length reduced significantly during •OH-induced apoptosis in HeLa cells. Again, GSH protects telomere from shortening (Fig. 5A).

Surprisingly, no inhibition in telomerase activity was observed throughout the •OH-induced apoptosis in HeLa, MW451 and 293 cells (Fig. 5B). The results are in accordance with a recent report regarding the cell killing by paclitaxol in murine melanoma cells [25], and etoposide, cisplatin, irinotecan, mitomycin and daunorubicin-mediated apoptosis in leukemic cells [26], as well as sodium butyrate-induced HeLa cell death [27].

3.4. Inhibition of telomerase activity increases susceptibility of HeLa cells to •OH-induced apoptosis

Although maintenance of telomerase activity does not protect tumor cells from •OH-induced cell killing in our systems, inhibition of telomerase with DODCB, a commonly used inhibitor of telomerase, caused an increased apoptosis at the same level of •OH. As shown in Fig. 6A, 20 μM DODCB caused a 90% decrease in telomerase activity. When HeLa cells were preincubated with 20 μM DODCB before treated with 0.1 mM $FeSO_4$/0.3 mM H_2O_2, apoptosis was significantly higher than control as detected by the TUNEL assay and flow cytometric analysis (Fig. 6B,C). The results suggest that inhibition of telomerase activity increased markedly the sensitivity of cells to apoptosis induction by •OH. Fig. 6D showed that more serious DNA laddering was observed when telomerase was inhibited. The results implicate that maintenance of telomerase activity is required for prevention of DNA damage and maintenance of tumor cell viability. It is

worth mentioning that DODCB alone does not cause cell death in HeLa cells and telomere shortening (data not shown). Our results suggest that telomere length but not telomerase activity plays a decisive role in apoptotic cell death under our experimental conditions.

3.5. *Caspase activation is not required in •OH-induced HeLa cell death*

We further asked if •OH-induced apoptosis is associated with the well-characterized caspase-related apoptotic pathway. In this study, we studied the effect of Ac-DEVD-CHO, a specific inhibitor of caspase-3 and caspase-7 to a certain extent, on •OH-induced apoptosis in HeLa cells. It was found that 0.1 mM Ac-DEVD-CHO showed no effect on DNA laddering (Fig. 7A) and the apoptotic cell death as detected by flow cytometric analysis (Fig. 7B). The nature of caspase-independent apoptosis induced by •OH was further verified by the assay of caspase-3 activity using a synthetic tetrapeptide Ac-DEVD-AMC (Ac-Asp-Glu-Val-Asp-7-amino-4-methyl coumarin) as a specific substrate. It was found that when 0.1 mM $FeSO_4$/0.3 mM H_2O_2 and 0.1 mM $FeSO_4$/0.6 mM H_2O_2 reaction were carried out to generate •OH, caspase-3 activity kept unchanged throughout the 24 h incubation (Fig. 7C). The results suggest that •OH-induced HeLa cell death is caspase-independent.

3.6. *•OH induces reduction of mitochondrial transmembrane potential ($\Delta\Psi_m$)*

Mitochondria are a physiological source of ROS generated by increased rate of respiration. It was found that ROS gen-

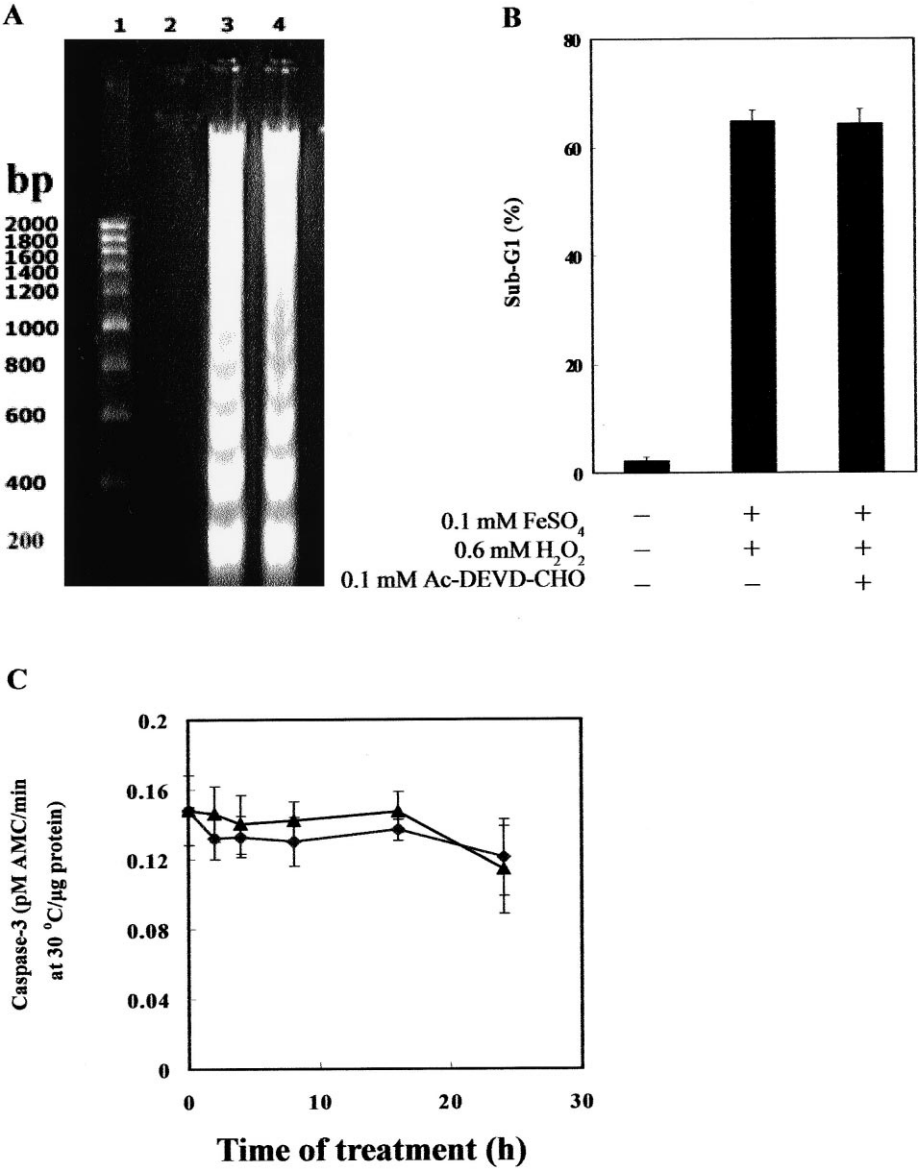

Fig. 7. Independence of caspase-3 in •OH-induced apoptotic HeLa cell death as evidenced by the inhibitor (Ac-DEVD-CHO) and study of caspase-3 activity assay. Cells were pretreated with 0.1 mM Ac-DEVD-CHO for 1 h before •OH treatment (0.1 mM $FeSO_4$/0.6 mM H_2O_2) and then analyzed by DNA laddering assay and flow cytometry. Caspase-3 activities were determined at different time points during •OH treatment. A: DNA laddering assay, lane 1: markers; lane 2: control; lane 3: DNA from •OH-treated cells; lane 4: DNA from cells pretreated with 0.1 mM Ac-DEVD-CHO. B: Flow cytometry assay. C: Caspase-3 activity during apoptosis induction. (▲) 0.1 mM $FeSO_4$/0.3 mM H_2O_2; (◇) 0.1 mM $FeSO_4$/0.6 mM H_2O_2. Values are means ± S.D. of three separate experiments done in triplicates. Error bars indicate standard deviations.

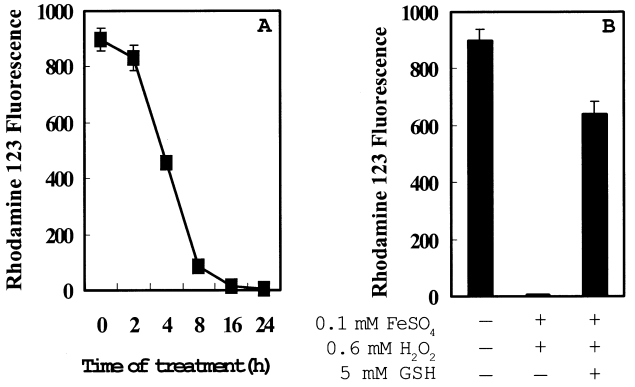

Fig. 8. Changes of $\Delta\Psi_m$ in •OH-treated HeLa cells as measured by Rh 123 staining. HeLa cells were treated with 0.1 mM $FeSO_4$/0.6 mM H_2O_2. A: Changes of $\Delta\Psi_m$ during apoptosis as analyzed by flow cytometry. B: Reduction of $\Delta\Psi_m$ by •OH treatment and the antagonistic effect of GSH. Values are means ± S.D. of three separate experiments done in triplicates. Error bars indicate standard deviations.

eration may cause opening of the MPT pores and loss of $\Delta\Psi_m$. In this study, we measured the change of $\Delta\Psi_m$ after •OH treatment in HeLa cells using Rh 123. We found that 8 h after •OH treatment, $\Delta\Psi_m$ was only 9.4% of that at zero time; 24 h after treatment, $\Delta\Psi_m$ was almost completely lost. Strikingly, when cells were pretreated with 5 mM GSH for 1 h before exposed to •OH, about a 71.3% recovery of $\Delta\Psi_m$ was observed (Fig. 8). Similar results were obtained using $DiOC_6(3)$ (Fig. 9). The results confirmed that changes of $\Delta\Psi_m$ were caused by free radicals.

Fig. 10 showed the time course of $\Delta\Psi_m$ reduction which was visualized by laser scan confocal microscopy. This event is thought to be mediated by the opening of the MPT pore which is regulated by ROS.

4. Discussion

It was found that ROS mediate apoptosis in various types of cells and under different conditions. In addition to the involvement of ROS in anti-cancer agent-induced apoptotic tumor cell death, ROS are reported to be involved in excitotoxic-, staurosporine-, and ceramide-induced neural cell death, ceramide-induced human leukemic U937 cell death, paraquat-induced death of endothelial cells, HIV-induced death of T cells and other apoptotic events [28–39]. However, the mechanisms underlying ROS-mediated apoptosis are far from being clarified.

In this study, we found that GSH can rescue •OH-induced apoptosis in HeLa cells. The results suggest an involvement of •OH functioning as ROS in the induction of apoptotic cell death. However, in addition to its function as an antioxidant, GSH also has other effects which may result in changes of protein folding and functions. To obtain more reliable evidence for the role of •OH in apoptosis, genetic overexpression of catalase should be a more suitable choice. More impor-

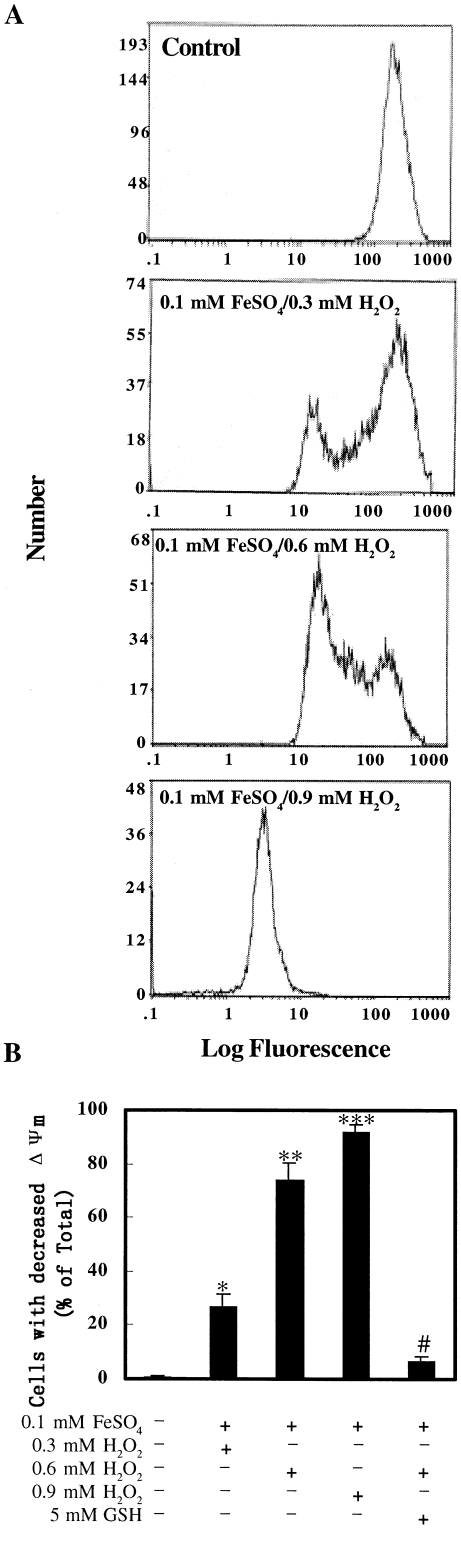

→

Fig. 9. •OH-induced reduction in $\Delta\Psi_m$ is concentration-dependent. HeLa cells were treated with different concentrations of Fe^{2+}/H_2O_2 for 16 h and measured by $DiOC_6(3)$ staining using flow cytometry. A: Cells were incubated in the absence or presence of Fe^{2+}/H_2O_2 in regular medium, labeled with $DiOC_6(3)$, and analyzed by flow cytometry. Representative recordings of six separate measurements are shown. The reduction in $\Delta\Psi_m$ in •OH-treated cells is evident from the decrease in the number of cells with the resting potential as well as from the appearance of the distinct peak of cells with lower $DiOC_6(3)$ fluorescence. After a 16 h treatment by 0.1 mM $FeSO_4$/0.9 mM H_2O_2, $\Delta\Psi_m$ was almost completely lost. B: Quantitation of the reduction $\Delta\Psi_m$ in •OH-induced apoptosis (means ± S.D., $n = 6$). $^*P < 0.05$; $^{**}P < 0.01$; $^{***}P < 0.001$ compared with the untreated group and $\#P < 0.05$ compared with the 0.1 mM $FeSO_4$/0.6 mM H_2O_2-treated group.

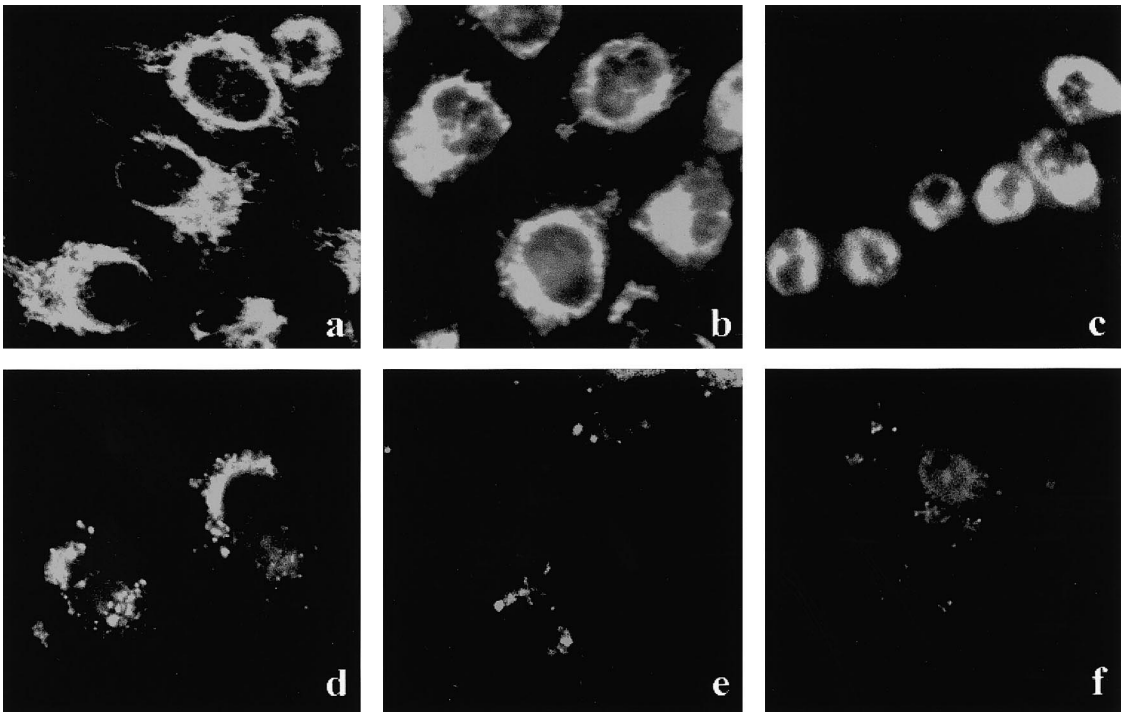

Fig. 10. Time course of $\Delta\Psi_m$ reduction during apoptosis as measured by Rh 123 staining and visualized by laser scan confocal microscopy. HeLa cells were treated with 0.1 mM $FeSO_4$/0.6 mM H_2O_2 for different time periods. a: 0 h; b: 2 h; c: 4 h; d: 8 h; e: 16 h; f: 24 h.

tantly, in our study we found that during •OH-induced apoptosis in HeLa cells telomere shortening occurs without inhibition of telomerase activity. The results suggest that ROS-induced telomere shortening is not through telomerase inhibition but possibly a direct effect of ROS on telomeres themselves. Using a chemical reaction system, Henle et al. [40] and Oikawa et al. [41] found that •OH-mediated DNA oxidations have preferential cleavage sites which are at the nucleoside 5′ to each of the dG moieties in the sequence RGGG, a sequence commonly found in telomeres. The results support the possibility that telomere may be a direct target of •OH. Furthermore, our finding that maintenance of normal telomerase activity did not prevent telomere shortening is quite interpretable. First, the rate of repairing of telomere by telomerase is not comparable with that of telomere shortening which is very dramatic and rapid. Second, it has been documented that telomerase alone is insufficient for telomere length maintenance, other factors are also required to stabilize telomere length [42].

Although telomerase inhibition is not required in •OH-induced apoptotic tumor cell death, telomerase-inhibited tumor cells are more susceptible to ROS. As shown in Fig. 6, when telomerase was inhibited by DODCB and the activity was only 12% of the original level, a 4-fold increase in percentage of apoptosis was observed in •OH-treated cells as compared with the control cells in which a normal telomerase activity was maintained. It is striking that DODCB alone without •OH treatment caused a very low level of apoptosis. This is in agreement with the data reported by Fu et al. [43] in PC12 cells. The results may have important implications for cancer chemotherapy since combinations of a telomerase inhibitor and an anti-cancer drug which induce ROS generation may be highly efficient in tumor cell killing.

On the other hand, in recent years, caspase-independent apoptotic cell death has been reported in different cell systems. One consistent feature of caspase-independent apoptosis is the loss or reduction of mitochondrial transmembrane potential ($\Delta\Psi_m$). Our results indicate that •OH-induced human tumor cell death is caspase-independent (Fig. 7) and is also associated with reduction of $\Delta\Psi_m$ (Figs. 8–10). More recently, apoptosis inducing factor (AIF), a caspase-independent effector of cell death, was characterized [44]. AIF locates in mitochondrial intermembrane space [44,45] and translocates to nucleus upon apoptosis induction leading to chromatin condensation, large scale of DNA fragmentation as well as $\Delta\Psi_m$ reduction [44]. Whether or not ROS affects AIF translocation is unclear at the present time. However, since MPT pore is sensitive to ROS, it is likely that ROS may stimulate AIF translocation. The interaction between ROS and AIF should be further scrutinized.

In summary, our study provides evidence that telomere shortening but not telomerase inhibition is the primary event during •OH-induced apoptosis in human tumor cells. We also found that ROS play a decisive role in human cell death by targeting directly at telomere and also mitochondria in someway affecting mitochondrial transmembrane potential and downstream events. Our study may have some implications for the strategy of development of cocktails of chemotherapeutic agents. For example, combinations of telomerase inhibitor and anti-cancer agent that generates ROS and shorten telomeres would be highly effective for cancer treatment.

References

[1] Simizu, S., Takada, M., Umezawa, K. and Imoto, M. (1998) J. Biol. Chem. 273, 26900–26907.
[2] Hockenbery, D.M., Oltvai, Z.N., Yin, X.-M., Milliman, C.L. and Korsmeyer, S.J. (1993) Cell 75, 241–251.

[3] Lafon, C., Mathieu, C., Guerrin, M., Pierre, O., Vidal, S. and Valette, A. (1996) Cell Growth Differ. 7, 1095–1104.
[4] Islam, K.N., Kayanoki, Y., Kantto, H., Suzuki, K., Asahi, M., Fujii, J. and Taniguchi, N. (1997) Free Radic. Biol. Med. 22, 1007–1017.
[5] Hoos, A., Hepp, H.H., Kaul, S., Ahlert, T., Bastert, G. and Wallwiener, D. (1998) Int. J. Cancer 79, 8–12.
[6] Herbert, B.-S., Pitts, A.E., Baker, S.I., Hamilton, S.E., Wright, W.E., Shay, J.W. and Corey, D.R. (1999) Proc. Natl. Acad. Sci. USA 96, 14276–14281.
[7] Zhang, X., Mar, V., Zhou, W., Harrington, L. and Robinson, M.O. (1999) Genes Dev. 13, 2388–2399.
[8] von Zglinicki, T., Saretzki, G., Docke, W. and Lotze, C. (1995) Exp. Cell Res. 220, 186–193.
[9] von Zglinicki, T., Pilger, R. and Sitte, N. (2000) Free Radic. Biol. Med. 28, 64–74.
[10] Decaudin, D., Marzo, I., Brenner, C. and Kroemer, G. (1998) Int. J. Oncol. 12, 141–152.
[11] Bossy-Wetzel, E., Newmeyer, D.D. and Green, D.R. (1998) EMBO J. 17, 37–49.
[12] Fulda, S., Scaffidi, C., Susin, S.A., Krammer, P.H., Kroemer, G., Peter, M.E. and Debatin, K.M. (1998) J. Biol. Chem. 273, 33942–33948.
[13] Kluck, R.M., Martin, S.J., Hoffman, B.M., Zhou, J.S., Green, D.R. and Newmeyer, D.D. (1997) EMBO J. 16, 4639–4649.
[14] Susin, S.A., Lorenzo, H.K., Zamzami, N., Marzo, I., Brenner, C. and Larochette, N. (1999) J. Exp. Med. 189, 381–394.
[15] Uehara, T., Kikuchi, Y. and Nomura, Y. (1999) J. Neurochem. 72, 196–205.
[16] Oexle, K. and Zwirner, A. (1997) Hum. Mol. Genet. 6, 905–908.
[17] Gavrieli, Y., Sherman, Y. and Ben-Sasson, S.A. (1992) J. Cell Biol. 119, 493–501.
[18] Mandal, M., Maggirwar, S.B., Sharmar, N., Kaufman, S.H., Sun, S.-C. and Kumar, R. (1996) J. Biol. Chem. 271, 30354–30359.
[19] Ishibashi, T. and Lippard, S.J. (1998) Proc. Natl. Acad. Sci. USA 95, 4219–4223.
[20] Hultdin, M., Grönlund, E., Norrback, K.-F., Eriksson-Lindström, E., Just, T. and Roos, G. (1998) Nucleic Acids Res. 26, 3651–3656.
[21] Rufer, N., Dragowska, W., Thornbury, G., Roosnek, E. and Lansdorp, P.M. (1998) Nat. Biotechnol. 16, 743–747.
[22] Yang, J., Liu, X., Bhalla, K., Kim, C.N., Ibrado, A.M., Cai, J., I-Peng, T., Jores, D.P. and Wang, X. (1997) Science 275, 1129–1132.
[23] Liu, D., Martino, G., Thargaraju, M., Sharma, M., Halwani, F., Shen, S.-H., Pate, Y.C. and Strikant, C.B. (2000) J. Biol. Chem. 275, 9244–9250.
[24] MacDonald, G., Shi, L., Velde, C.V., Lieberman, J. and Greenberg, A.H. (1999) J. Exp. Med. 189, 131–143.
[25] Multani, A.S., Li, C., Ozem, M., Imam, A.S., Wallace, S. and Pathak, S. (1999) Oncol. Rep. 6, 39–44.
[26] Akiyama, M., Horiguchiyamada, J., Saito, S., Hoshi, Y., Yamada, D., Mizoguchi, H. and Yamada, H. (1999) Eur. J. Cancer 35, 309–315.
[27] Ren, J.G., Xia, H.L. and Dai, Y.R. (2000) Chin. Sci. Bull. 45, 1861–1866.
[28] Buttke, T.M. and Sandstrom, P.A. (1995) Free Radic. Res. 22, 389–397.
[29] Patel, M., Day, B.J., Crapo, J.D., Fridovich, I. and McNamara, J.O. (1996) Neuron 16, 345–355.
[30] Dobmeyer, T.S., Findhammer, S., Dobmeyer, J.M., Klein, S.A., Raffel, B., Hoelzer, D., Helm, E.B., Kabelitz, D. and Rossol, R. (1997) Free Radic. Biol. Med. 22, 775–785.
[31] Fadeel, B., Ahlin, A., Henter, J.I., Orrenius, S. and Hampton, M.B. (1998) Blood 92, 4808–4818.
[32] Shimmura, S., Masumizu, T., Nakai, Y., Urayama, K., Shimazaki, J., Bissen-Miyajima, H., Kohno, M. and Tsubota, K. (1999) Invest. Ophthalmol. Vis. Sci. 40, 1245–1249.
[33] Foresti, R., Sarathchandra, P., Clark, J.E., Green, C.J. and Motterlini, R. (1999) Biochem. J. 339, 729–736.
[34] Chen, C., Wei, T.T., Gao, Z.H., Zhao, B.L., Hou, J.W., Xu, H.B., Xin, W.J. and Packer, L. (1999) Biochem. Mol. Bol. Int. 47, 397–405.
[35] Ishikawa, Y., Satoh, T., Enokido, Y., Nishio, C., Ikeuchi, T. and Hatanaka, H. (1999) Brain Res. 824, 71–80.
[36] Liu, R.G., Narla, R.K., Kurinov, I., Li, B.L. and Uckun, F.M. (1999) Radiat. Res. 151, 133–141.
[37] Rolletlabelle, E., Grange, M.J., Elbim, C., Marquetty, C., Gougerotpocidalo, M.A. and Pasquier, C. (1998) Free Radic. Biol. Med. 24, 563–572.
[38] Li, P.F., Dietz, R. and Vonharsdorf, R. (1997) Circulation 96, 3602–3609.
[39] Deas, O., Dumont, C., MacFarlane, M., Rouleau, M., Hebib, C., Harper, F., Hirsch, F., Charpentier, B., Cohen, G.M. and Senik, A. (1998) J. Immunol. 161, 3375–3383.
[40] Henle, E.S., Han, Z., Tang, N., Rai, P., Luo, Y. and Linn, S. (1999) J. Biol. Chem. 274, 962–971.
[41] Oikawa, S. and Kawanishi, S. (1999) FEBS Lett. 453, 365–368.
[42] McEacherm, M.J. and Blackburn, E.H. (1996) Genes Dev. 10, 1822–1834.
[43] Fu, W., Begley, J.W., Killen, M.W. and Mattson, M.P. (1999) J. Biol. Chem. 274, 7264–7271.
[44] Susin, S.A., Lorenzo, H.K., Zamzami, N., Marzo, I., Show, B.E., Brothers, G.M., Mangion, J., Jacotot, E., Costantini, P., Loeffler, M., Larochette, N., Goodlett, D.R., Aebersold, R., Siderovski, D.P., Enninger, J.M. and Kroemer, G. (1999) Nature 397, 441–446.
[45] Lorenzo, H.K., Susin, S.A., Penninger, J. and Kroemer, G. (1999) Cell Death Differ. 6, 516–526.